

# RMAU-NET: A Residual-Multihead-Attention U-Net Architecture for Landslide Segmentation and Detection from Remote Sensing Images

Lam Pham\*, Cam Le\*, Hieu Tang\*, Khang Truong\*, Truong Nguyen, Jasmin Lampert, Alexander Schindler, Martin Boyer, Son Phan<sup>†</sup>

**Abstract**—In recent years, landslide disasters have reported frequently due to the extreme weather events of droughts, floods, storms, or the consequence of human activities such as deforestation, excessive exploitation of natural resources. However, automatically observing landslide is challenging due to the extremely large observing area and the rugged topography such as mountain or highland. This motivates us to propose an end-to-end deep-learning-based model which explores the remote sensing images for automatically observing landslide events. By considering remote sensing images as the input data, we can obtain free resource, observe large and rough terrains by time. To explore the remote sensing images, we proposed a novel neural network architecture which is for two tasks of landslide detection and landslide segmentation. We evaluated our proposed model on three different benchmark datasets of LandSlide4Sense, Bijie, and Nepal. By conducting extensive experiments, we achieve F1 scores of 98.23, 93.83 for the landslide detection task on LandSlide4Sense, Bijie datasets; mIoU scores of 63.74, 76.88 on the segmentation tasks regarding LandSlide4Sense, Nepal datasets. These experimental results prove potential to integrate our proposed model into real-life landslide observation systems.

**Items**— Attention, landslide detection, landslide segmentation, remote sensing image, U-Net.

## I. INTRODUCTION

According to the literature, landslides often occur due to the instability of slopes [1], [2], [3]. During such events, soil, rock, mud, or debris from geological activities collapse and slide out/down from hills or mountains, causing significant damage across multiple aspects of human life, including loss of life, psychological trauma after suffering the event, demolishing of agriculture, and long-term impacts on communities near the affected sites [4]. For example, a landslide in the Indian state of Kerala in July 2024 resulted in 24 fatalities [5], while another landslide in Ethiopia during the same month claimed 257 lives [6].

To address the issue of landslides, a common approach involves the creation of landslide inventory maps, which store timestamp, location, and type of the event [7]. In addition, to look ahead landslide events and provide early warning, landslide inventory maps can be built from various data sources,

including aerial imagery from satellites [8], elevation models, and LiDAR altimetry [9]. Analyzing landslide by exploring normal images require high cost and skilled investigators who would verify images with tools and experience to delineate landslide boundaries [10]. The output could be a finalized map where landslide areas are annotated with different colors, or it could undergo further analysis using Geographic Information Systems (GIS) software, facilitated by advancements in geospatial technology [7]. Generally, this process, which heavily depends on human expertise, presents several challenges. Firstly, the low quality of given images in landslide-prone regions can compromise the accuracy of the mapping process, as it is time-consuming and labor-intensive. Secondly, experts often rely on specific ‘signatures’, such as topological differences [11], [12] or the principle that ‘the past and present are keys to the future’ [13], [14], to identify landslide sites. The manual selection of these properties may lead to inconsistent results among researchers and could potentially overlook unknown factors contributing to future landslide occurrences.

Thanks to advancements in Earth Observation (EO) technologies, these techniques have significantly enhanced the accessibility and prevalence of remote sensing data from satellites such as Sentinel and Landsat [15]. These advancements include the introduction of multiple spectral bands capable of covering a wide range of visible wavelengths, with Sentinel-2 offering up to 13 bands, and the WorldView-3 satellite achieving a resolution as fine as 0.31 meters per pixel [16]. Additionally, the rapid proliferation of unmanned aerial vehicles (UAVs) [17] has established these technologies as mainstream tools in the study of landslide phenomena. Furthermore, recent emergence of machine learning and deep learning has introduced innovative quantitative assessment methodologies for addressing the problem of landslide inventory mapping [18]. Through iterative learning processes utilizing existing datasets, machine learning and deep learning models can uncover latent relationships between input data features and corresponding outcomes, providing implicit solutions for landslide segmentation without the necessity of designing complex mathematical models.

In recent years, research has often focused on traditional machine learning models such as Support Vector Machines (SVM) [20], [21], Artificial Neural Networks (ANN) [20], [22], and Random Forest (RF) [23], [20]. However, there is a notable shift in research trends toward deep learning models, such as U-Net [24], [25], [26], DeepLab [27], and transformers [28], [29], which are inspired by computer vi-

L. Pham is with Van Lang University, Vietnam.

L. Pham, C. Le, J. Lampert, A. Schindler, and M. Boyer are with the Competence Unit Data Science & Artificial Intelligence at the Austrian Institute of Technology, Austria.

H. Tang is with the Troyes University, France.

K. Truong and T. Nguyen are with HCM University of Technology, Vietnam.

S. Phan is with Ton Duc Thang University, Vietnam.

(\*) Main and equal contribution into the paper.

(†) Corresponding author.

TABLE I  
BANDS' INFORMATION IN LANDSLIDE4SENSE DATASET [19]

Band	Centre $\lambda$ (nm)	Spatial resolution $\Delta \lambda$ (m)	Description
Band 1	443	60	Atmospheric correction (aerosol scattering)
Band 2	490	10	Sensitive to vegetation senescing, carotenoid, browning and soil background; atmospheric correction (aerosol scattering)
Band 3	560	10	Green peak, sensitive to total chlorophyll in vegetation
Band 4	665	10	Maximum chlorophyll absorption
Band 5	705	20	Position of red edge; consolidation of atmospheric corrections/ fluorescence baseline.
Band 6	740	20	Position of red edge, atmospheric correction, retrieval of aerosol load.
Band 7	783	20	Leaf Area Index (LAI)
Band 8	842	10	Edge of the Near-Infrared (NIR) plateau
Band 9	945	60	Water vapour absorption, atmospheric correction.
Band 10	1375	60	Detection of thin cirrus for atmospheric correction. Sensitive to lignin, starch
Band 11	1610	20	and forest above ground biomass. Snow/ice /Scldoud separation.
Band 12	1610	20	Assessment of Mediterranean vegetation conditions. Distinction of clay soils for the monitoring of soil erosion. Distinction between live biomass, dead biomass and soil, e.g. for burn scars mapping.

sion segmentation problems and often yield superior results. For instance, a comparative study on segmentation tasks in the Rasuwa district of the Himalayas demonstrated that the best machine learning model (a variant of Random Forest) achieved an F1 score of 82.07% and a mean Intersection over Union (mIoU) score of 69.6%, while the top-performing deep learning model attained an F1 score of 87.8% and an mIoU score of 78.26% [30]. This indicates that deep-learning-based architectures perform more advances and prove potential for further improvement. However, almost published papers for landslide detection or segmentation from remote sensing image, in which deep-learning-based models were proposed, used their own data from various resources or different settings [31], [32], [33], [34], [35], [36]. As these data were self-collected and has not published, this lead challenges to compare models' performance. Additionally, authors focused on landslide events in certain regions which present different natural backgrounds. These reasons causes challenges to evaluate cross-datasets which prevents the model development and evaluation.

Inspired by deep-learning approach and address the concerns mentioned above, we propose a deep-learning-based model for landslide detection and segmentation tasks by exploring remote sensing images in this paper. We mainly contribute:

- We conducted extensive experiments to indicate the role of deep-learning techniques such as input features, network architectures, loss functions, etc. which are used to construct a deep-learning-based model for landslide segmentation. Given the experimental results, we proposed a novel network architecture, referred to as RMAU-NET, which achieved the high performance on both tasks of landslide detection and segmentation.
- To prove the proposed network architecture robust, we

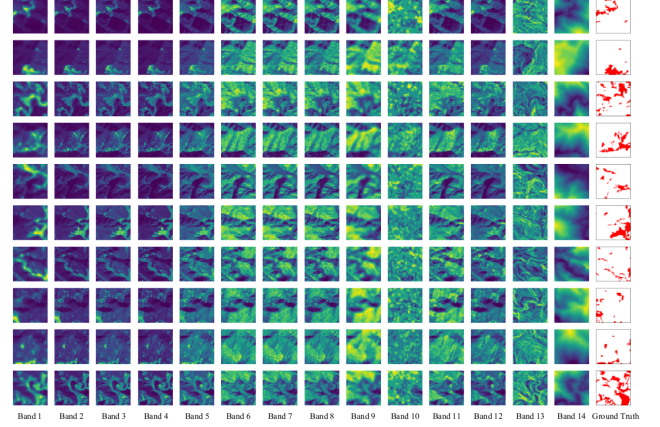


Fig. 1. Some image samples with 14 band and corresponding mask from Landslide4Sense dataset [19]

TABLE II  
STATISTICS OF REMOTE SENSING IMAGES DATASETS FOR LANDSLIDE DETECTION OR SEGMENTATION

Datasets	Image Number	Image Size	Landslide Image Ratio	Landslide Pixel Ratio	Proposed Tasks
Landslide4Sense [19]	3044	128×128×14	58%	2.3%	Segmentation
Bijie [37]	2773	128×128×3	27%	3.9%	Detection
Nepal [38]	275	128×128 ×3	-	0.8%	Segmentation

evaluate on three published and benchmark datasets of LandSlide4Sense [19], Bijie [37], and Nepal [38]. The experimental results present our proposed model potential to integrate into real-life landslide observation systems.

The remainder of this paper is structured as follows: Section II describes remote sensing image (RSI) datasets proposed for landslide detection or segmentation. Given the RSI datasets, we define our tasks, suggest the evaluation metrics, data splitting, and present experimental settings in this section. Section III presents our proposed baseline which is evaluated on the benchmark dataset of Landslide4Sense for the segmentation task. Given the baseline in Section III, we evaluate a wide range of deep-learning techniques to further improve the baseline, achieving a novel network for both tasks of landslide detection and segmentation in Section IV. Section IV evaluates our proposed network on different datasets of Landslide4Sense, Bijie, and Nepal, and then our proposed network is compared with the state-of-the-art systems. Finally, Section V concludes the paper.

## II. REMOTE SENSING IMAGE DATASETS AND TASK DEFINITION

As the paper focuses on landslide detection and segmentation from remote sensing images, we first collect published and benchmark remote sensing image (RSI) datasets which involve in landslide events. As our knowledge, there are three largest datasets proposed for landslide detection segmentation which have been published until now. These are Landslide4Sense [19], Bijie [37], and Nepal [38]. Given these selected RSI datasets, we define two tasks of landslide detection and landslide segmentation, the evaluation metrics, dataset splitting, and experimental settings in this paper.

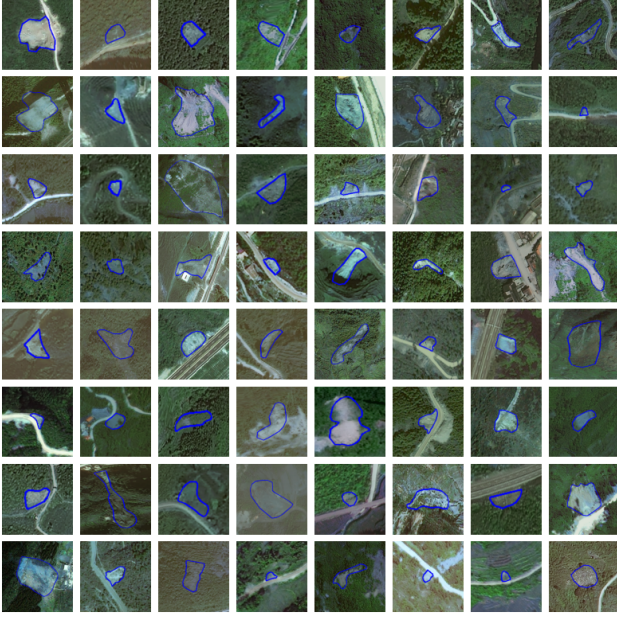


Fig. 2. Some image samples from Bijie dataset [37]

#### A. Remote sensing image datasets

**Landslide4Sense dataset [19]** illustrates landslide appearances worldwide from 2015 to 2021. This dataset provides as an essential benchmark for analyzing landslide disaster in regions with heavy rainfall, earthquakes, or unstable geological conditions. The entire Landslide4Sense dataset comprises 3844 multi-spectral images each of which is a combination of 14 bands. In particular, bands from B1 to B12 (12 bands) are from the Sentinel-2 which are comprehensively described in Table I. B13 band is from slope data and B14 band was taken from the ALOS PALSAR satellite. Each band presents the same size of  $128 \times 128$  and the mask data presents a binary image with the same dimensions of  $128 \times 128$ . While white pixels in the mask indicate landslide-affected areas, black pixels indicate non-landslide areas. Additionally, each pixel in each layer corresponds to a real-world scale of 10 to 60 meters. Some image samples with 14 bands and the corresponding masks are comprehensively shown in Fig. 1. According to the statistics of Landslide4Sense dataset as shown in Table II, the number of image contains landslide regions is approximately 58% of all images in the dataset. However, the number of landslide region only take 2.3% of all pixels in the dataset. This presents a significant imbalance between landslide and none-landslide regions which leads challenging to segmentation models.

**Bijie dataset [37]:** This dataset was collected from Triple-Sat Satellite for Bijie City, northwest of Guizhou Province, with an area of  $26,853 \text{ km}^2$ . The elevation of this region is from 457m to 2,900m combining with unstable geology and heavy rainfall, making it severe landslide location in China. After collecting from the satellite, the images are transformed into RGB format which presets the size of  $128 \times 128 \times 3$ . Fig. 2 illustrates some RGB image samples

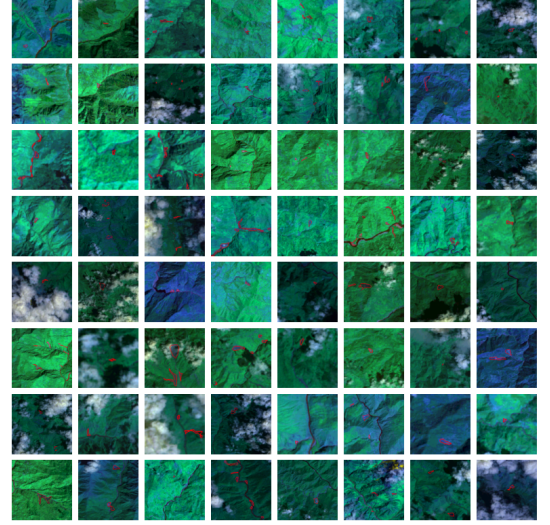


Fig. 3. Some image samples from Nepal Dataset [38]

from the dataset (i.e., The blue lines in each image mark landslide regions). In total, the Bijie dataset comprises 770 landslide images. Additionally, the dataset includes 2,003 images of none-landslide regions in Bijie city. This indicates an imbalance between landslide and none-landslide image samples. Regarding landslide and none-landslide pixels, the statistics in Table II presents a ratio of 3.9/96.1 which shows a significant imbalance and same as Landslide4Sense dataset.

**Nepal [38]:** To collect the data, geologists first extract locations and time of landslide events. Given these information, remote sensing images from Landsat-8 satellite were obtained and manually verified. Same as Bijie dataset, the collected images from the satellite were transformed into RGB format with the size of  $128 \times 128 \times 3$ . Some image samples are shown in Fig. 3. Totally, Nepal dataset [38] comprises 230 images with landslide events. According to statistics in Table II, the total number of landslide pixels is very small, only 0.8% of the entire dataset which present a significant imbalance regarding pixel level.

#### B. Task definition

Given the published remote sensing image datasets which involve in landslide events, it reveals that each dataset was proposed for either landslide detection or landslide segmentation. Indeed, published papers using the Nepal dataset have omitted the segmentation task [38], [39], [40] as this dataset only provides remote sensing images with landslide regions. In contrast, the Bijie dataset includes a significant number of non-landslide images, which led to the primary focus on classification task in relevant papers of [37], [41], [42]. Regarding Landslide4Sense dataset, it was proposed for a challenge and the competition metrics are for the landslide segmentation task [43], [19]. This inspires us to evaluate our proposed model on both tasks of landslide detection and segmentation on Bijie and Landslide4Sense datasets, and only segmentation task on then Nepal dataset.



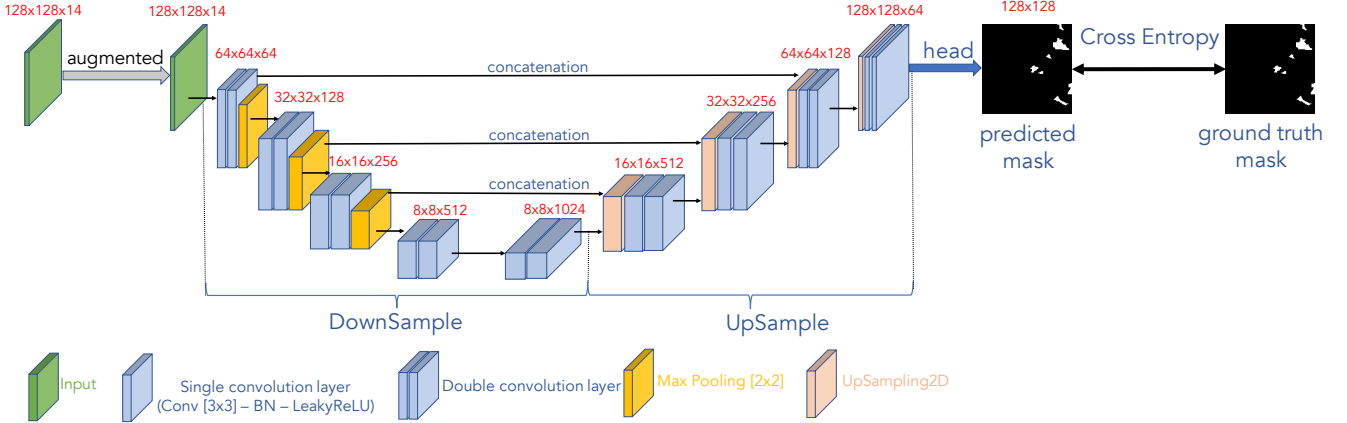


Fig. 4. The proposed U-Net baseline architecture for the landslide segmentation.

Compare among these datasets, it can be seen that Landslide4Sense presents the largest image number with a balance landslide/none-landslide image. The dataset also show diverse landslide region collected from various places over the world. We, therefore, select Landslide4Sense dataset to evaluate our proposed baseline. We then further improve the baseline by applying and evaluating various deep-learning techniques such as input features, network architecture, loss function, post-processing, etc. Given evaluation results, we propose the best model configuration for both tasks of landslide detection and segmentation. We then evaluate the best model on the remaining datasets of Bijie, Nepal, and compare with the state-of-the-art systems.

### C. Dataset splitting

As the Landslide4Sense dataset [19] has not published the label of test set (800 images). We split the training set (3044 images) into two parts, using an 80:20 ratio, for training and testing, respectively. For the Bijie dataset [37], we omit the suggestion in the paper [41], remaining the 70:30 ratio for the train and test sets. Regarding Nepal dataset [38], it was suggested to divide the entire dataset into training, validation, and test sets. Hence, we omit this suggestion and keep the training and validation sets for model development while the test set is used for the evaluation.

### D. Evaluation metrics

To evaluate our proposed model, we report the F1-score, Precision, Recall, and the mean Intersection over Union (mIoU) on the pixel level for the segmentation task. Regarding the detection task, F1-score, Precision, and Recall on the image level are provided.

### E. Experimental settings

We construct our proposed deep neural networks with Tensorflow framework. All deep neural networks are trained for 30 epochs on Titan RTX 24GB gpu. All evaluating models in this paper use Adam [44] for the optimization in the training process.

## III. THE PROPOSED BASELINE MODEL

As mentioned in Section II-B, we first propose a baseline model for landslide segmentation and evaluate multiple deep-learning techniques with the baseline on Landslide4Sense dataset. As shown in Fig. 4, the baseline consists of three main components: The online data augmentation, the U-Net backbone network architecture, and the head with the loss function for the segmentation task.

### A. The online data augmentation

Given input remote sensing images, we first apply two data augmentation methods of rotation and cutmix. In particular, each image is randomly rotated using angles of 90, 180, or 270 degrees to generate a new images, referred to as the rotation augmentation. Then, landslide regions from random landslide images are cut and mixed with the current processing image, referred to as the cutmix augmentation [45]. As these two data augmentation methods are applied on batch of remote sensing images during the training process, we referred to as the online data augmentation.

### B. The U-Net based backbone architecture

As Fig. 4 shows, the U-Net backbone consists of the downsample and upsample networks. Both downsample and upsample networks leverage the double convolutional architectures. Each of double convolutional architecture presents two single convolutional layers performing a convolutional layer (Conv), batchnorm layer (BN) [46], and Leaky Rectifine Linear Unit (LeakyReLU) [47] in the order. For down-sampling, MaxPooling layer is applied. Meanwhile, UpSampling2D layer is used for up-sampling.

### C. The head and loss function

Given the output feature map of  $128 \times 128 \times 64$  from the U-Net backbone, a global average pooling layer across the channel dimension is applied to obtain the predicted mask of  $128 \times 128$ . The predicted mask is then compared with the ground truth mask using Cross-Entropy loss function

TABLE III

EVALUATE THE PROPOSED BASELINE ON LANDSLIDE4SENSE DATASET WITH THE SEGMENTATION TASK

Network	F1 score	mIoU
U-Net baseline	67.83	60.01

TABLE IV

EVALUATE THE EFFECT OF THE LOSS FUNCTIONS.

Networks & Loss	F1 score	mIoU
U-Net & Cross Entropy (baseline)	67.83	60.01
U-Net & Focal Loss	<b>68.28</b>	<b>60.37</b>
U-Net & Log-Cosh Loss	67.73	59.95
U-Net & IoU Loss	<b>68.20</b>	<b>60.23</b>
U-Net & Tversky Loss	66.21	58.54
U-Net & Lovasz Loss	64.61	57.37
U-Net & Boundary Loss	60.14	54.92
U-Net & Center Loss	65.61	58.21
U-Net & Focal & IoU Loss	<b>69.05</b>	<b>61.14</b>

$$Loss_{EN}(\theta) = -\frac{1}{N} \sum_{i=1}^N y_i \cdot \log \{\hat{y}_i(\theta)\} + \frac{\lambda}{2} \cdot \|\theta\|_2^2 \quad (1)$$

where  $Loss(\theta)$  is the loss function over all trainable parameters  $\theta$ , constant  $\lambda$  is set to 0.0001,  $y_i$  and  $\hat{y}_i$  are expected and predicted  $N = 16384$  pixels from the feature map of  $128 \times 128$ .

#### D. Evaluate the proposed baseline on Landslide4Sense dataset

We evaluate the proposed baseline on Landslide4Sense dataset with the segmentation task. To this end, we first train the proposed baseline. After the training process, we feed the test images of  $128 \times 128 \times 14$  into the baseline, obtain the predicted mask. The predicted mask is then compared with the ground truth, compute the F1 and mIoU scores on the pixel level. As Table IV shows, the baseline achieves F1 and mIoU scores of 67.83 and 60.01, respectively.

### IV. EVALUATE DEEP LEARNING TECHNIQUES TO IMPROVE THE BASELINE

Given the baseline, we now conduct extensive experiments applying a wide range of deep-learning techniques of loss function, input features, network architectures, optimization algorithms, and post processing methods in the order. We evaluate whether these techniques are effective to further improve the baseline performance.

#### A. Evaluate loss functions

Among deep-learning techniques mentioned above, we first evaluate the role of loss functions. We tackle the imbalance issue between landslide pixels and non-landslide pixels in the segmentation task by evaluating a wide range of loss functions of Focal loss [48], Log-Cosh loss [49], IoU loss [50], Tversky loss [51], Lovasz loss [52], Boundary loss [53], and Center loss [54]. While the online data augmentation and U-Net backbone in the proposed baseline are remained, the Cross-Entropy loss in the head is replaced by the loss functions in Table IV to perform the segmentation task on Landslide4Sense dataset.

TABLE V

NEW BAND DATA IS GENERATED FROM 14 ORIGINAL BANDS IN LANDSLIDE4SENSE DATASET.

New band data	Formula / Method
Band 15 to Band 17	$(x - x_{min}) / (x_{max} - x_{min})$
Band 18: NDVI	$(B8 - B4) / (B8 + B4)$
Band 19: NDMI	$(B8 - B11) / (B8 + B11)$
Band 20: NBR	$(B8 - B12) / (B8 + B12)$
Band 21: Gray	$(B2 + B3 + B4) / 3$
Band 22 to Band 23	Gaussian and Median filters
Band 24 to Band 25	Image gradients across length and width
Band 26	Canny Edge detector

TABLE VI

EVALUATE THE EFFECT OF THE INPUT FEATURE (U-Net\*: U-Net BASELINE WITH THE COMBINED LOSS FUNCTION).

Network & band data	F1 score	mIoU
U-Net* & Original 14 bands	69.05	61.14
U-Net* & Original 14 bands & bands 15 to 17	69.39	61.22
U-Net* & Original 14 bands & bands 15 to 21	69.83	60.97
U-Net* & Original 14 bands & bands 15 to 23	<b>69.96</b>	<b>61.76</b>
U-Net* & Original 14 bands & bands 15 to 25	69.91	61.64
U-Net* & Original 14 bands & bands 15 to 26	68.54	60.65

As the experimental results shown in Table VI, Focal loss and IoU loss outperform the other loss functions. This inspires us to combine both Focal loss and IoU loss. The combination of Focal loss and IoU loss is defined by

$$Loss = \alpha \cdot Loss_{Focal} + (1 - \alpha) \cdot Loss_{IoU}, \quad (2)$$

where  $\alpha$  presents the portion between two loss functions, which is empirically set to 0.5. Compare to the baseline with Cross-Entropy loss, the combination of Focal loss and IoU loss yields improvements of 1.22 regarding the F1-score and 1.13 for the mIoU score.

#### B. Evaluate input feature

Inspired by [55], we evaluate whether generating band data is effective to enrich the features of remote sensing images, then improving the segmentation performance. Therefore, we generate 12 new band data from the 14 original bands of a remote sensing image in Landslide4Sense dataset. The methods used to generate new band data are presented in Table V and summarized by:

- Bands 15 to 17 are generated by applying RGB normalization on bands B2, B3 and B4.
- Bands 18 to 21 represent remote sensing indices (NDVI, NDMI, NBR) and a grayscale image.
- Bands 22 and 23 are generated by applying Gaussian and median filters with kernel size of  $[10 \times 10]$ .
- Bands 24 and 25 are calculated from the image gradient (across length and width dimensions).
- Band 26 presents the result of using Canny edge detector.

As the experimental results are shown in Table VI, it indicates that adding generating band data is effective to improve the performance of the segmentation task. Particularly, adding bands from 15 to 23 presents the most significant improvement of 0.91 and 0.62 for F1 score and mIoU score, respectively.

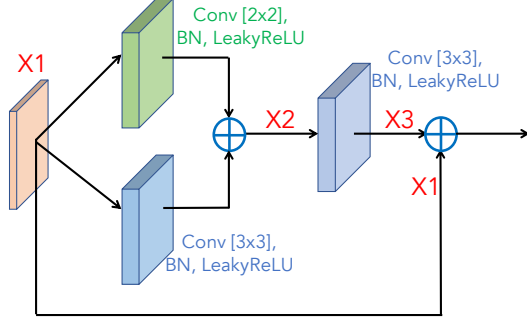


Fig. 5. The proposed Residual-Convolutional layer.

TABLE VII

EVALUATE THE EFFECT OF THE MULTIPLE HEADS (U-Net+: U-Net BASELINE WITH 23 BAND DATA AND COMBINED LOSS FUNCTION).

Network	F1 score	mIoU
U-Net+	69.96	61.76
U-Net+ & Multiple heads	<b>70.45</b>	<b>62.19</b>

### C. Evaluate the network architectures

Regarding the network architecture, we propose two main improvements: (1) The proposed multiple head resolution instead of the single head architecture in the baseline; (2) The combination of residual-convolutional and attention layers to replace the traditional convolutional layer in U-Net backbone. The detailed improvements are comprehensive described in the Fig. 4.

For the first improvement, we are inspired by applying an ensemble of multiple predicted masks with different resolutions to enhance the system performance. In particular, instead of using only one head block to generate one predicted mask of  $128 \times 128$ , we add two more head blocks to generate two other predicted masks:  $256 \times 256$  and  $64 \times 64$ . As a result, the final predicted result is obtained from an average of three predicted output masks. The experimental result on Landslide4Sense dataset shown in Table VII indicates that applying multiple heads helps to enhance the segmentation performance, further improving 0.49 and 0.53 on F1 score and mIoU score, respectively. Notably, this experiment remains the advances of 23 band data and the combination of Focal and IoU loss functions in previous experiments.

Regarding the U-Net backbone, we first evaluate whether U-Net based architecture is the most effective model for the segmentation task. In particular, we replace the U-Net backbone by Deeplab-V3 [56], MobileNet-V3 [57] and EfficientNet-V2 [58] architectures. Secondly, we are inspired that the multiple kernel sizes and a residual based architecture is more effective to capture distinct features of feature maps rather than a conventional convolutional layer. We therefore develop an architecture of a residual-convolutional layer (Res-Conv) as shown in Fig. 5 which is used to replace the double convolution layer in both the downsample and upsample architecture in the baseline.

We further improve the network architecture by applying an attention layer after every convolutional layer in both

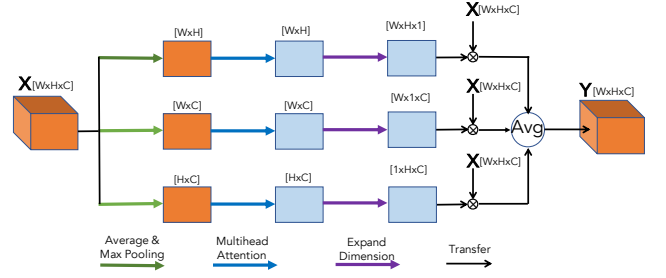


Fig. 6. The proposed multihead-attention layer.

TABLE VIII

EVALUATE THE NETWORK ARCHITECTURE IMPROVEMENTS (U-Net+: U-Net BASELINE WITH 23 BAND DATA, COMBINED LOSS FUNCTION, AND MULTIPLE RESOLUTION HEADS).

Networks	F1 score	mIoU
U-Net+	70.45	62.19
DeepLab-V3	68.30	60.49
MobileNet-V3	60.26	54.72
EfficientNet-V2	64.51	57.27
U-Net+ & CBAM Att.	70.82	62.53
U-Net+ & SE Att.	71.26	62.86
U-Net+ & Multihead Att.	71.45	63.05
U-Net+ & Res-Conv	72.07	63.45
U-Net+ & Multihead Att. & Res-Conv	<b>72.42</b>	<b>63.88</b>

the downsample and upsample architectures. The attention weights generated by the proposed attention layer effectively enforces the neural network to focus on landslide regions on the feature maps inside the network. We evaluate three types of attention schemes: SE [59] attention, CBAM [60] attention, and our proposed multi-head attention in our published paper [61]. Rather than only focusing on certain dimension of a feature map, our proposed multi-head attention as shown in Fig. 6 explores all three dimensions of the feature map. In particular, given an input feature map  $\mathbf{X}$  with a size of  $[W \times H \times C]$  where  $W$ ,  $H$ , and  $C$  presents width, height, and channel dimensions, the feature map  $\mathbf{X}$  is reduced size across three dimensions using both max and average pooling layers, generating new two-dimensional feature maps. Then, the traditional multi-head attention [62] is applied to each two-dimensional feature maps before multiplying with the original three-dimensional feature map  $\mathbf{X}$ .

As the experimental results are shown in Table VIII, U-Net based architecture is more effective than evaluating network architectures of DeepLab-V3, MobileNet-V3, EfficientNet-V2. Regarding applying attention and Res-Conv layer, both techniques help to improve the segmentation performance. When these techniques are combined, it helps to improve F1 score and mIoU score by 1.97 and 1.69 respectively. Notable, this experiment reuses the advances of previous experimental results with using 23 band data, combined loss function, and multiple resolution heads

### D. Evaluate post processing

Given the advances of using 23 band data, combined loss function, multiple resolution heads, and combination of multihead attention and Res-Conv layer regarding U-Net

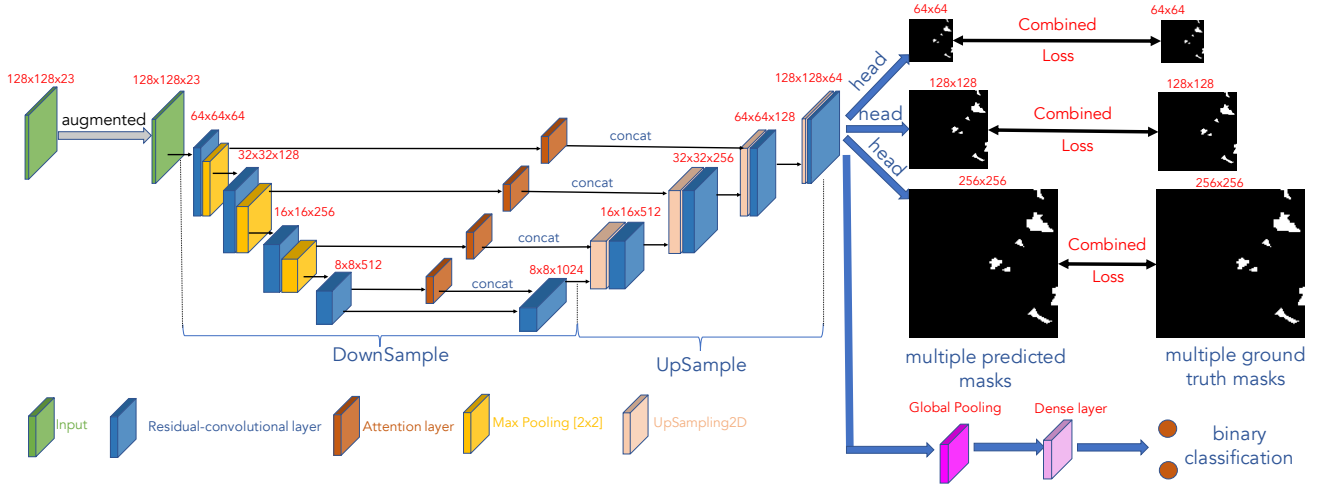


Fig. 7. The proposed RMAU-NET architecture.

TABLE IX  
EVALUATE THE THRESHOLD VALUES

Threshold Values	F1 score	mIoU
None	72.42	63.88
0.4	71.78	63.29
0.5	72.42	63.88
0.6	72.60	64.02
0.75	73.02	64.43
0.85	73.13	64.69
0.9	73.68	65.07
<b>0.95</b>	<b>74.63</b>	<b>65.97</b>
0.99	73.11	64.68

backbone, we finally evaluate the role of post processing step. In particular, we apply a threshold value to decide whether a pixel is referred to as the landslide or none-landslide. The Table IX indicates that we obtained the best F1 score of 74.463 and mIoU score of 65.97 at the threshold value of 0.95.

#### V. PROPOSE RMAU-NET FOR LANDSLIDE DETECTION AND SEGMENTATION

As the extensive experiments were conducted above, we indicate that leveraging multiple deep-learning techniques of combined loss (IoU loss and Focal loss), 23 band data (8 generating band data and 14 original band data), multiple resolution heads, a combination of Res-Conv layer and our proposed multihead attention layer, and post-processing with certain threshold shows effective to further improve the segmentation performance. The Table X comprehensively describes the improvement from each technique with the significant enhancement from network architecture improvement (applying Res-Conv layer and Multihead attention layer) and threshold-based post-processing.

Given these advanced techniques, we propose a novel network architecture for both tasks of landslide segmentation and detection, referred to as RMAU-NET. As the novel network is shown in Fig. 8, all advanced deep learning techniques, which are evaluated in the previous section, are applied. To adapt the landslide detection task, the global

pooling layer is applied on the feature map of  $128 \times 128 \times 64$  before flattening, and going through a dense layer for the binary classification of landslide and none-landslide. The proposed RMAU-NET is then evaluated with other datasets of Bijie [37], and Nepal [38], achieving the state-of-the-art results on both landslide detection and segmentation tasks as shown in Table XI. Some segmentation results obtained from RMAU-NET model on LandSlide4Sense dataset are also shown in Fig. 8

#### VI. CONCLUSION

We have presented a deep-learning-based approach for landslide detection and segmentation from remote sensing imagery. By evaluating the effects of various improvements of feature engineering, network architecture, loss functions, optimization algorithms, and post processing, we finally construct the RMAU-NET which bases on U-Net architecture. The extensive experiments prove that our proposed RMAU-NET is robust on different benchmark datasets of Landslide4Sense, Bijie, and Nepan which shows potential to apply for remote-sensing-image-based landslide analysis systems.

#### REFERENCES

- [1] The International Charter Space and Major Disasters, "Landslides," <https://disasterscharter.org/web/guest/disaster-types/-/article/landslides>, Accessed: August 25, 2024.
- [2] Luciano Picarelli, Suzanne Lacasse, and Ken KS Ho, "The impact of climate change on landslide hazard and risk," *Understanding and Reducing Landslide Disaster Risk: Volume 1 Sendai Landslide Partnerships and Kyoto Landslide Commitment 5th*, pp. 131–141, 2021.
- [3] EM-DAT, "The international emergency disasters database," 2023.
- [4] Thomas Glade and Michael J. Crozier, *The Nature of Landslide Hazard Impact*, chapter 2, pp. 41–74, John Wiley & Sons, Ltd, 2005.
- [5] The International Charter Space and Major Disasters, "Landslide in india," <https://disasterscharter.org/web/guest/activations/-/article/landslide-in-india-activation-900->, Accessed: August 25, 2024.

TABLE X

APPLY DEEP LEARNING TECHNIQUES TO FURTHER IMPROVE THE U-NET BASELINE FOR LANDSLIDE SEGMENTATION ON LANDSLIDE4SENSE DATASET

Network	Combined loss	23 band data	Multiple heads	Res-Conv & Multihead Att.	Threshold	F1 score	mIoU
U-Net w/	-	-	-	-	-	67.83	60.01
U-Net w/	✓	-	-	-	-	69.05	61.14
U-Net w/	✓	✓	-	-	-	69.96	61.76
U-Net w/	✓	✓	✓	-	-	70.45	62.19
U-Net w/	✓	✓	✓	✓	-	72.42	63.88
U-Net w/	✓	✓	✓	✓	✓	74.63	65.97

TABLE XI

PERFORMANCE COMPARISON ON LANDSLIDE4SENSE, NEPAL, AND BIJIE DATASETS

Dataset	Model	Segmentation Task				Detection Task			
		F1 score	Precision	Recall	mIoU	F1 Score	Accuracy	Precision	Recall
Landslide4Sense	Our proposed RMAU-NET	76.90	72.11	82.38	65.97	98.23	97.10	98.58	97.89
Nepal	ResNet [38]	60.00	55.00	65.00	n/a	n/a	n/a	n/a	n/a
	U-Net [38]	67.00	61.00	74.00	n/a	n/a	n/a	n/a	n/a
	Our proposed RMAU-NET	69.43	62.12	78.79	76.88	n/a	n/a	n/a	n/a
Bijie	DDTL [37]	n/a	n/a	n/a	n/a	n/a	79.69	n/a	n/a
	DDTL+SE [37]	n/a	n/a	n/a	n/a	n/a	93.36	n/a	n/a
	DDTL+CBAM [37]	n/a	n/a	n/a	n/a	n/a	95.89	n/a	n/a
	Improved DDTL [37]	n/a	n/a	n/a	n/a	n/a	96.03	n/a	n/a
	Our proposed RMAU-NET	74.34	74.54	74.14	57.33	93.83	96.63	95.52	92.21

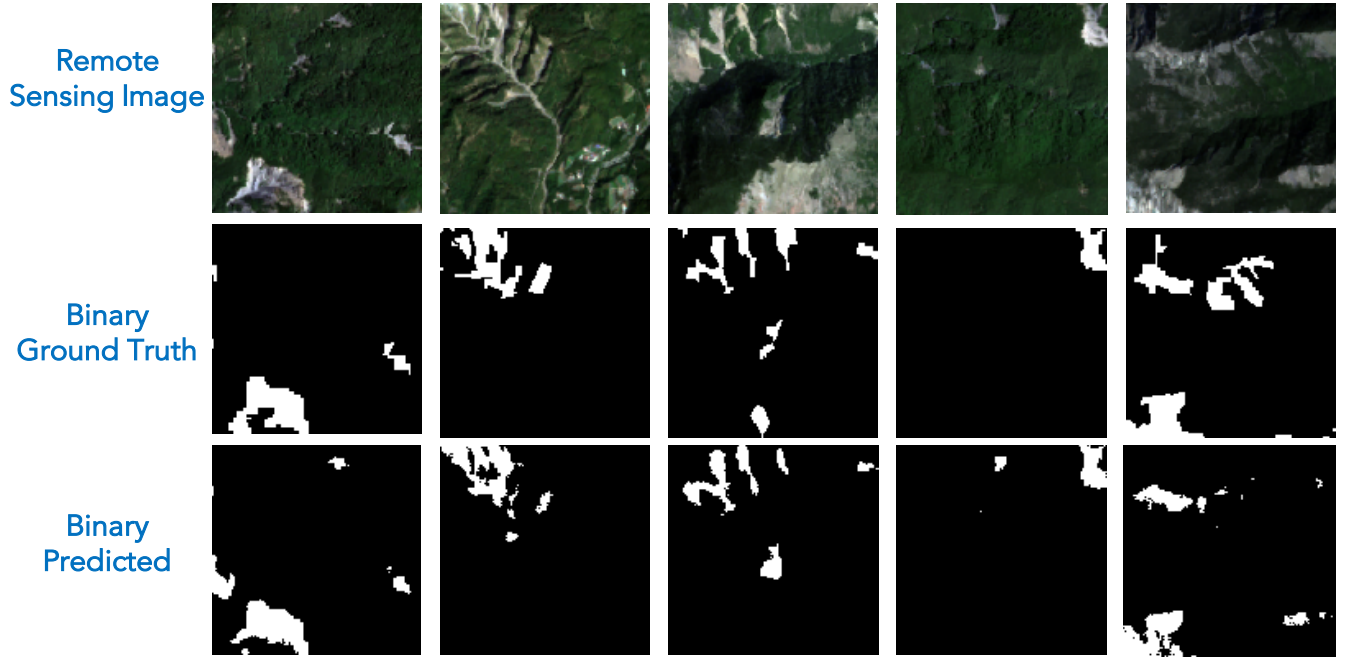


Fig. 8. Segmentation results obtained from RMAU-NET model on Landslide4Sense remote sensing images.

- [6] The International Charter Space and Major Disasters, "Landslide in ethiopia," <https://disasterscharter.org/web/guest/activations/-/article/landslide-in-ethiopia-activation-899->, Accessed: August 25, 2024.
- [7] Fausto Guzzetti, Alessandro Cesare Mondini, Mauro Cardinali, Federica Fiorucci, Michele Santangelo, and Kang-Tsung Chang, "Landslide inventory maps: New tools for an old problem," *Earth-Science Reviews*, vol. 112, no. 1-2, pp. 42–66, 2012.
- [8] Zhongbin Li, Wenzhong Shi, Ping Lu, Lin Yan, Qunming Wang, and Zelang Miao, "Landslide mapping from aerial photographs using change detection-based markov random field," *Remote Sensing of Environment*, vol. 187, pp. 76–90, Dec. 2016.
- [9] J McKean and J Roering, "Objective landslide detection and surface morphology mapping using high-resolution airborne laser altimetry," *Geomorphology*, vol. 57, no. 3-4, pp. 331–351, 2004.
- [10] Cees J Van Westen, Enrique Castellanos, and Sekhar L Kuriakose, "Spatial data for landslide susceptibility, hazard, and vulnerability assessment: An overview," *Engineering geology*, vol. 102, no. 3-4, pp. 112–131, 2008.
- [11] Nancy F. Glenn, David R. Streutker, D. John Chadwick, Glenn D. Thackray, and Stephen J. Dorsch, "Analysis of lidar-derived topographic information for characterizing and differentiating landslide morphology and activity," *Geomorphology*, vol. 73, no. 1, pp. 131–148, 2006.
- [12] Oliver Korup, John J. Clague, Reginald L. Hermanns, Kenneth Hewitt, Alexander L. Strom, and Johannes T. Weidinger, "Giant landslides, topography, and erosion," *Earth and Planetary Science Letters*, vol. 261, no. 3, pp. 578–589, 2007.
- [13] Heping Shu, Marcel Hürlimann, Roberto Molowny-Horas, Marta



- González, Jordi Pinyol, Clàudia Abancó, and Jinzhu Ma, "Relation between land cover and landslide susceptibility in val d'aran, pyrenees (spain): Historical aspects, present situation and forward prediction," *Science of The Total Environment*, vol. 693, pp. 133557, 2019.
- [14] L. Pisano, V. Zumpano, Ž. Malek, C.M. Roskopf, and M. Parise, "Variations in the susceptibility to landslides, as a consequence of land cover changes: A look to the past, and another towards the future," *Science of The Total Environment*, vol. 601-602, pp. 1147-1159, 2017.
- [15] Qiang Zhao, Le Yu, Zhenrong Du, Dailiang Peng, Pengyu Hao, Yongguang Zhang, and Peng Gong, "An overview of the applications of earth observation satellite data: impacts and future trends," *Remote Sensing*, vol. 14, no. 8, pp. 1863, 2022.
- [16] Ava Vali, Sara Comai, and Matteo Matteucci, "Deep learning for land use and land cover classification based on hyperspectral and multispectral earth observation data: A review," *Remote Sensing*, vol. 12, no. 15, pp. 2495, 2020.
- [17] Emilien Alvarez-Vanhard, Thomas Corpetti, and Thomas Houet, "Uav & satellite synergies for optical remote sensing applications: A literature review," *Science of remote sensing*, vol. 3, pp. 100019, 2021.
- [18] Amrita Mohan, Amit Kumar Singh, Basant Kumar, and Ramji Dwivedi, "Review on remote sensing methods for landslide detection using machine and deep learning," *Transactions on Emerging Telecommunications Technologies*, vol. 32, no. 7, pp. e3998, 2021.
- [19] Omid Ghorbanzadeh, Yonghao Xu, Hengwei Zhao, Junjie Wang, Yanfei Zhong, Dong Zhao, Qi Zang, Shuang Wang, Fahong Zhang, Yilei Shi, Xiao Xiang Zhu, Lin Bai, Weile Li, Weihang Peng, and Pedram Ghamisi, "The outcome of the 2022 landslide4sense competition: Advanced landslide detection from multisource satellite imagery," *IEEE Journal of Selected Topics in Applied Earth Observations and Remote Sensing*, vol. 15, pp. 9927-9942, 2022.
- [20] Taskin Kavzoglu, Ismail Colkesen, and Emrehan Kutlug Sahin, "Machine learning techniques in landslide susceptibility mapping: a survey and a case study," *Landslides: Theory, practice and modelling*, pp. 283-301, 2019.
- [21] Gowtham Rajmohan, Chandru Vignesh Chinnappan, Alfred Daniel John William, Sivaparthipan Chandrakrishnan Balakrishnan, Bala Anand Muthu, and Gunasekaran Manogaran, "Revamping land coverage analysis using aerial satellite image mapping," *Transactions on Emerging Telecommunications Technologies*, vol. 32, no. 7, pp. e3927, 2021.
- [22] Soyoung Park, Chuluong Choi, Byungwoo Kim, and Jinsoo Kim, "Landslide susceptibility mapping using frequency ratio, analytic hierarchy process, logistic regression, and artificial neural network methods at the inje area, korea," *Environmental earth sciences*, vol. 68, pp. 1443-1464, 2013.
- [23] Tao Chen, John C Trinder, and Ruiqing Niu, "Object-oriented landslide mapping using zy-3 satellite imagery, random forest and mathematical morphology, for the three-gorges reservoir, china," *Remote sensing*, vol. 9, no. 4, pp. 333, 2017.
- [24] Chaoyang Niu, Ouyang Gao, Wanjie Lu, Wei Liu, and Tao Lai, "Regsa-unet++: A lightweight landslide detection network based on single-temporal images captured postlandslide," *IEEE Journal of Selected Topics in Applied Earth Observations and Remote Sensing*, vol. 15, pp. 9746-9759, 2022.
- [25] Hesheng Chen, Yi He, Lifeng Zhang, Sheng Yao, Wang Yang, Yumin Fang, Yaoliang Liu, and Binghai Gao, "A landslide extraction method of channel attention mechanism u-net network based on sentinel-2a remote sensing images," *International Journal of Digital Earth*, vol. 16, no. 1, pp. 552-577, 2023.
- [26] Ximing Chen, Xin Yao, Zhenkai Zhou, Yang Liu, Chuangchuang Yao, and Kaiyu Ren, "Drs-unet: A deep semantic segmentation network for the recognition of active landslides from insar imagery in the three rivers region of the qinghai-tibet plateau," *Remote Sensing*, vol. 14, no. 8, pp. 1848, 2022.
- [27] Bowen Du, Zirong Zhao, Xiao Hu, Guanghui Wu, Liangzhe Han, Leilei Sun, and Qiang Gao, "Landslide susceptibility prediction based on image semantic segmentation," *Computers & Geosciences*, vol. 155, pp. 104860, 2021.
- [28] Renxiang Huang and Tao Chen, "Landslide recognition from multi-feature remote sensing data based on improved transformers," *Remote Sensing*, vol. 15, no. 13, pp. 3340, 2023.
- [29] Han Fu, Bihong Fu, and Pulong Shi, "An improved segmentation method for automatic mapping of cone karst from remote sensing data based on deeplab v3+ model," *Remote Sensing*, vol. 13, no. 3, pp. 441, 2021.
- [30] Omid Ghorbanzadeh, Thomas Blaschke, Khalil Gholamnia, Sansar Raj Meena, Dirk Tiede, and Jagannath Aryal, "Evaluation of different machine learning methods and deep-learning convolutional neural networks for landslide detection," *Remote Sensing*, vol. 11, no. 2, pp. 196, 2019.
- [31] Guilherme Pereira Bento Garcia, LP Soares, Mateus Espadoto, and Carlos Henrique Grohmann, "Relict landslide detection using deep-learning architectures for image segmentation in rainforest areas: a new framework," *International Journal of Remote Sensing*, vol. 44, no. 7, pp. 2168-2195, 2023.
- [32] Trong-An Bui, Pei-Jun Lee, Kai-Yew Lum, Clarissa Loh, and Kyo Tan, "Deep learning for landslide recognition in satellite architecture," *IEEE Access*, vol. 8, pp. 143665-143678, 2020.
- [33] Sepideh Tavakkoli Piralilou, Hejar Shahabi, Ben Jarihani, Omid Ghorbanzadeh, Thomas Blaschke, Khalil Gholamnia, Sansar Raj Meena, and Jagannath Aryal, "Landslide detection using multi-scale image segmentation and different machine learning models in the higher himalayas," *Remote Sensing*, vol. 11, no. 21, pp. 2575, 2019.
- [34] Vanessa Böhm, Wei Ji Leong, Ragini Bal Mahesh, Ioannis Prapas, Edoardo Nemni, Freddie Kalaitzis, Siddha Ganju, and Raul Ramos-Pollan, "Sar-based landslide classification pretraining leads to better segmentation," *arXiv preprint arXiv:2211.09927*, 2022.
- [35] Zhenyu Zhao, Shucheng Tan, Yiquan Yang, and Qinghua Zhang, "Landslide identification from post-earthquake high-resolution remote sensing images based on resnet-bfa," *Remote Sensing*, vol. 17, no. 6, pp. 995, 2025.
- [36] Meng Tang, Yuelin He, Muhammed Aslam, Edore Akpokodje, and Syeda Fizzah Jilani, "Enhanced u-net++ for improved semantic segmentation in landslide detection," *Sensors*, vol. 25, no. 9, pp. 2670, 2025.
- [37] Shunping Ji, Dawen Yu, Chaoyong Shen, Weile Li, and Qiang Xu, "Landslide detection from an open satellite imagery and digital elevation model dataset using attention boosted convolutional neural networks," *Landslides*, vol. 17, pp. 1337-1352, 2020.
- [38] L. Bragagnolo, L.R. Rezende, R.V. da Silva, and J.M.V. Grzybowski, "Convolutional neural networks applied to semantic segmentation of landslide scars," *CATENA*, vol. 201, pp. 105189, 2021.
- [39] Fang Chen, Bo Yu, and Bin Li, "A practical trial of landslide detection from single-temporal landsat8 images using contour-based proposals and random forest: A case study of national nepal," *Landslides*, vol. 15, pp. 453-464, 2018.
- [40] Bo Yu, Fang Chen, and Chong Xu, "Landslide detection based on contour-based deep learning framework in case of national scale of nepal in 2015," *Computers & Geosciences*, vol. 135, pp. 104388, 2020.
- [41] Shengwu Qin, Xu Guo, Jingbo Sun, Shuangshuang Qiao, Lingshuai Zhang, Jingyu Yao, Qiushi Cheng, and Yanqing Zhang, "Landslide detection from open satellite imagery using distant domain transfer learning," *Remote sensing*, vol. 13, no. 17, pp. 3383, 2021.
- [42] Yongxin Li, Zhihui Xin, Guisheng Liao, Penghui Huang, and Mengting Yuan, "Landslide detection for remote sensing images using a multi-label classification network based on bijie landslide dataset," *IEEE Journal of Selected Topics in Applied Earth Observations and Remote Sensing*, 2024.
- [43] Omid Ghorbanzadeh, Yonghao Xu, Pedram Ghamisi, Michael Kopp, and David Kreil, "Landslide4sense: Reference benchmark data and deep learning models for landslide detection," *IEEE Transactions on Geoscience and Remote Sensing*, vol. 60, pp. 1-17, 2022.
- [44] P. K. Diederik and B. Jimmy, "Adam: A method for stochastic optimization," *CoRR*, vol. abs/1412.6980, 2015.
- [45] Sangdoo Yun, Dongyoon Han, Seong Joon Oh, Sanghyuk Chun, Junsuk Choe, and Youngjoon Yoo, "Cutmix: Regularization strategy to train strong classifiers with localizable features," in *Proceedings of the IEEE/CVF international conference on computer vision*, 2019, pp. 6023-6032.
- [46] Sergey I. and Christian S., "Batch normalization: Accelerating deep network training by reducing internal covariate shift," in *Proc. ICML*, 2015, pp. 448-456.
- [47] Andrew L Maas, Awni Y Hannun, Andrew Y Ng, et al., "Rectifier nonlinearities improve neural network acoustic models," in *Proc. ICML*, 2013, vol. 30, p. 3.
- [48] Tsung-Yi Lin, Priya Goyal, Ross Girshick, Kaiming He, and Piotr Dollár, "Focal loss for dense object detection," *IEEE Transactions on Pattern Analysis and Machine Intelligence*, vol. 42, no. 2, pp. 318-327, 2020.

- [49] Qi Wang, Yue Ma, Kun Zhao, and Yingjie Tian, "A comprehensive survey of loss functions in machine learning," *Annals of Data Science*, pp. 1–26, 2020.
- [50] Hamid Rezaatofghi, Nathan Tsoi, JunYoung Gwak, Amir Sadeghian, Ian Reid, and Silvio Savarese, "Generalized intersection over union: A metric and a loss for bounding box regression," in *Proc. CVPR*, 2019, pp. 658–666.
- [51] Seyed Sadegh Mohseni Salehi, Deniz Erdogmus, and Ali Gholipour, "Tversky loss function for image segmentation using 3d fully convolutional deep networks," in *International workshop on machine learning in medical imaging*. Springer, 2017, pp. 379–387.
- [52] Jiaqian Yu and Matthew B Blaschko, "The lovász hinge: A novel convex surrogate for submodular losses," *IEEE transactions on pattern analysis and machine intelligence*, vol. 42, no. 3, pp. 735–748, 2018.
- [53] Alexey Bokhovkin and Evgeny Burnaev, "Boundary loss for remote sensing imagery semantic segmentation," in *International Symposium on Neural Networks*, 2019, pp. 388–401.
- [54] Yandong Wen, Kaipeng Zhang, Zhifeng Li, and Yu Qiao, "A comprehensive study on center loss for deep face recognition," *International Journal of Computer Vision*, vol. 127, pp. 668–683, 2019.
- [55] Ruyin Cao, Yang Chen, Miaogen Shen, Jin Chen, Ji Zhou, Cong Wang, and Wei Yang, "A simple method to improve the quality of ndvi time-series data by integrating spatiotemporal information with the savitzky-golay filter," *Remote Sensing of Environment*, vol. 217, pp. 244–257, 2018.
- [56] Liang-Chieh Chen, "Rethinking atrous convolution for semantic image segmentation," *arXiv preprint arXiv:1706.05587*, 2017.
- [57] Siying Qian, Chenran Ning, and Yuepeng Hu, "Mobilenetv3 for image classification," in *2021 IEEE 2nd International Conference on Big Data, Artificial Intelligence and Internet of Things Engineering (ICBAIE)*, 2021, pp. 490–497.
- [58] Brett Koonce and Brett Koonce, "Efficientnet," *Convolutional neural networks with swift for Tensorflow: image recognition and dataset categorization*, pp. 109–123, 2021.
- [59] Jie Hu, Li Shen, and Gang Sun, "Squeeze-and-excitation networks," in *Proc. CVPR*, June 2018.
- [60] Sanghyun Woo, Jongchan Park, Joon-Young Lee, and In So Kweon, "Cbam: Convolutional block attention module," in *Proc. ECCV*, 2018, pp. 3–19.
- [61] Cam Le, Lam Pham, Jasmin Lampert, Matthias Schlögl, and Alexander Schindler, "Landslide detection and segmentation using remote sensing images and deep neural networks," in *IGARSS 2024 - 2024 IEEE International Geoscience and Remote Sensing Symposium*, 2024, pp. 9582–9586.
- [62] Ashish Vaswani, Noam Shazeer, Niki Parmar, Jakob Uszkoreit, Llion Jones, Aidan N Gomez, Łukasz Kaiser, and Illia Polosukhin, "Attention is all you need," *Advances in neural information processing systems*, vol. 30, 2017.